

## Control of the charge-transfer interaction between a flexible porous coordination host and aromatic guests by framework isomerism<sup>†</sup>

Yohei Takashima,<sup>ab</sup> Shuhei Furukawa<sup>\*bc</sup> and Susumu Kitagawa<sup>\*abc</sup>

Received 13th February 2011, Accepted 22nd March 2011

DOI: 10.1039/c1ce05201b

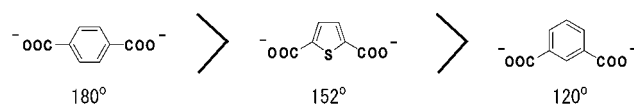
Based on 2,5-thiophenedicarboxylate (thdc), two isomorphic frameworks,  $[\text{Zn}(\text{thdc})(\text{dpNDI})]_n$ , are assembled from zinc ions and *N,N'*-di(4-pyridyl)-1,4,5,8-naphthalenediimide (dpNDI). Because of the significant difference in their porous structures, these isomers show different charge-transfer interactions with electron-donating aromatic molecules.

Porous coordination polymers (PCPs),<sup>1</sup> which are assembled using metal ions as nodes and organic ligands as linkers, are an intriguing class of porous materials that have been vigorously studied for applications in storage<sup>2</sup> and separation.<sup>3</sup> This is because their designable framework architectures provide confined spaces that selectively and efficiently trap specific gas molecules, such as hydrogen,<sup>4</sup> acetylene,<sup>5</sup> and carbon dioxides.<sup>6</sup> The pore surface designability of PCPs using strategic organic chemistry provides a further opportunity to incorporate redox-active organic molecules as the framework scaffold for a potential application as colorimetric sensors, especially when the redox-active module interacts with a guest species confined in the pores, to produce a charge-transfer (CT) transition that can be modulated by the redox potential of the guest molecules.<sup>7</sup> One of the advantages of using PCPs is that the individual redox-active molecules are aligned with spatial regularity, which prevents preferential aggregation. Therefore, the alignment of organic linkers and the resulting pore structure can be controlled by topological design of the frameworks,<sup>8</sup> which enables altering of the conformation of the trapped guest species and the CT interaction between the redox-active module and the guest molecule.

The design of the framework topology relies both on the geometry of the metal ions and on the connecting angle of the organic linkers.

In this sense, 2,5-thiophenedicarboxylate (thdc) can work as a topology-directing ligand because of its unique connecting angle (152°), as seen in the middle of two well-known dicarboxylate linkers: terephthalate (tpa, 180°) and isophthalate (isa, 120°), as shown in Scheme 1. Therefore, thdc is expected to induce the formation of two different framework isomers that were originally composed of either tpa or isa, respectively. These dicarboxylate linkers are often used simultaneously with diamine linkers to construct porous frameworks; tpa forms a three-dimensional (3D) pillared-layer framework and isa forms an interdigitated two-dimensional (2D) framework, a so-called CID, where CID = coordination polymer with an interdigitated structure.<sup>9,10</sup> We introduced *N,N'*-di(4-pyridyl)-1,4,5,8-naphthalenediimide (dpNDI) as a diamine linker with redox-active properties. Because dpNDI has an electron-accepting ability, it is possible to form CT complexes with electron-donating guest molecules<sup>11</sup> incorporated into the pores. Here, we report two topological isomers of PCPs with thdc and dpNDI. The conformation of thdc induces either an isa-type 2D framework or a tpa-type 3D framework. The resulting frameworks show different colorimetric properties arising from the structural dimensionality and flexibility.

A 3D framework of  $\{[\text{Zn}(\text{thdc})(\text{dpNDI})]\cdot 6\text{DMF}\}_n$  (**1**  $\supset$  **DMF**) was synthesized from the reaction of  $\text{Zn}(\text{NO}_3)_2 \cdot 6\text{H}_2\text{O}$ ,  $\text{H}_2\text{thdc}$  and dpNDI in a DMF solution at 393 K. Single-crystal X-ray diffraction analysis<sup>‡</sup> showed that **1**  $\supset$  **DMF** has a pillared-layer structure, where dimeric Zn ions are bridged by four thdc moieties to form the 2D layer structure, followed by connecting layers of dpNDI at the axial positions of the Zn ions, as shown in Fig. 1 and 3. As a result, the Zn ions have a unique trigonal bipyramidal geometry. An analogous structure with 2,5-dihydroxyterephthalate (dhytpa) and 4,4'-bipyridine (bpy) has been reported as  $[\text{Zn}(\text{dhytpa})(\text{bpy})]$ , where the dhytpa and Zn ions form a 2D layer and the bpy is the pillar ligand.<sup>12</sup> The 2D layer of **1**  $\supset$  **DMF** is flatter than  $[\text{Zn}(\text{dhytpa})(\text{bpy})]$ , although the dimeric Zn moieties are similar to each other (Fig. 3a and b). The dihedral angle between the octagon motif of the dimeric Zn moiety and the thiophene or phenylene rings is 0° and 14.12° for **1**  $\supset$  **DMF** and 16.77° for  $[\text{Zn}(\text{dhytpa})(\text{bpy})]$ , respectively. The void volume,



**Scheme 1** The angles between two carboxylates for tpa, thdc and isa.

<sup>a</sup>Department of Synthetic Chemistry and Biological Chemistry, Graduate School of Engineering, Kyoto University, Katsura, Nishikyo-ku, Kyoto, 615-8510, Japan. E-mail: kitagawa@sbchem.kyoto-u.ac.jp; Fax: +81-75-383-2732; Tel: +81-75-383-2733

<sup>b</sup>ERATO Kitagawa Integrated Pores Project, Japan Science and Technology Agency (JST), Kyoto Research Park bldg #3, Shimogyo-ku, Kyoto, 600-8815, Japan. E-mail: shuhei.furukawa@kip.jst.go.jp; Fax: +81-75-325-3572; Tel: +81-75-322-4711

<sup>c</sup>Institute for Integrated Cell-Material Sciences, Kyoto University, Yoshida, Sakyo-ku, Kyoto, 606-8501, Japan

<sup>†</sup> Electronic supplementary information (ESI) available: Experimental details, thermogravimetric analyses, and PXRD. CCDC reference numbers 782568 and 782567. For ESI and crystallographic data in CIF or other electronic format see DOI: 10.1039/c1ce05201b

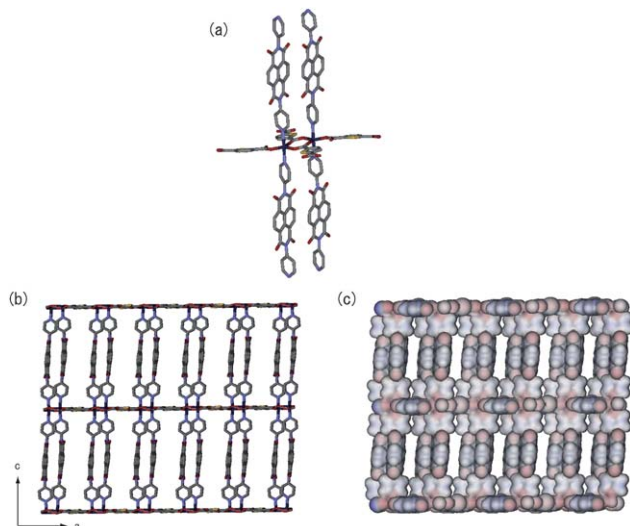


**Fig. 1** Crystal structure of **1**·DMF showing (a) coordination environment of Zn(II) ion and (b) pillared layer structure. Gray, blue, red, yellow, and navy are C, N, O, S and Zn, respectively. The hydrogen atoms and guest molecules are omitted for clarity. (c) VDW surface colored by the interpolated charge.

$V_{\text{void}}$  is 62.7% of the total crystal volume, calculated using the PLATON software package. Thermogravimetric analysis of **1**·DMF showed the release of DMF molecules from the cavities with increasing temperature up to 423 K. No further weight loss was observed up to 533 K (see ESI†, Fig. S1).

By contrast, the 2D CID-type framework of  $\{[\text{Zn}(\text{thdc})(\text{dpNDI})]\cdot 10\text{MeOH}\cdot 2\text{DMF}\}_n$  (**2**·DMF·MeOH) was synthesized by simply changing the solvent system from DMF to a mixture of DMF/MeOH. Single-crystal X-ray diffraction analysis showed the existence of a similar dimeric Zn moiety to **1**·DMF which was connected by four thdc molecules to produce a one-dimensional (1D) double-chain structure of  $\{[\text{Zn}(\text{thdc})]\}_n$  along the [100] direction, followed by a connection of the chains by dpNDI in the axial position of the Zn ions to give a 2D layer motif. The 2D layers are mutually interdigitated to create a 3D assembled porous framework (Fig. 2). The structure of **2**·DMF·MeOH consists of two types of intersecting linear pores, in which five methanol and one DMF molecules are accommodated. The void volume,  $V_{\text{void}}$ , is 33.5% of the total crystal volume. Thermogravimetric analysis of **2**·DMF·MeOH showed a stepwise release of solvent, indicating that five methanol and one DMF molecules were released up to 403 K (see ESI†, Fig. S2).

A series of CID structures has been reported with bpy as the diamine linker and a variety of dicarboxylic acids with connecting angles of 120°. Examples are isophthalate derivatives, benzophenone-4,4'-dicarboxylate, and 2,7-naphthalene dicarboxylate. Note that whereas the coordination environment of the Zn ions and the resulting Zn dimer structure of **1** and **2** are similar to each other, the shapes constructed by the two Zn ions and the two carboxylate moieties differ. In **1** the shape is octagonal and in **2** it is hexagonal, as shown in Fig. 3. The coordination angle of the C–O–Zn bond in the polygons is 131.5(2)° and 157.6(2)° for **1** and 113.9(3)° and 170.4(3)° for **2**. Interestingly, all the reported CID structures have hexagonal Zn dimer moieties and this unique dimer structure seems to be essential for obtaining the 1D double-chain structure. Moreover, a significant difference in the molecular orientation was observed for

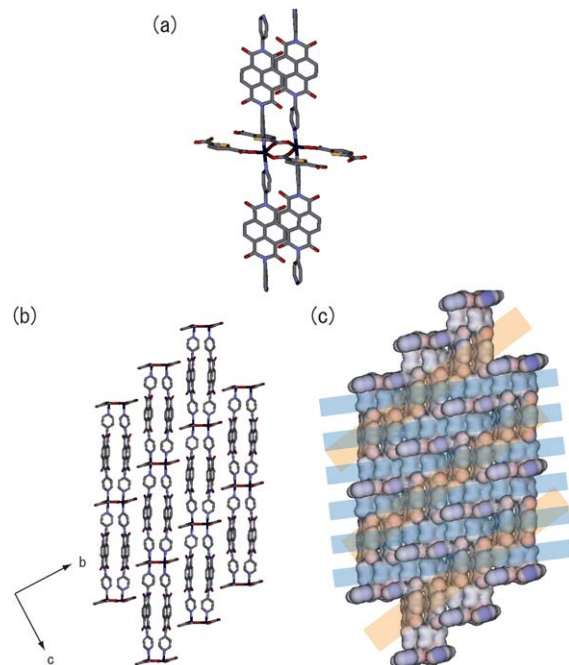


**Fig. 2** Crystal structure of **2**·DMF·MeOH showing (a) coordination environment of Zn(II) ion and (b) 3D assembled framework with 2D layer structures. Gray, blue, red, yellow, and navy are C, N, O, S and Zn, respectively. The hydrogen atoms and guest molecules are omitted for clarity. (c) VDW surface colored by the interpolated charge. Blue and orange lines mean the intersecting linear pores.

thdc, which does not participate in the formation of the polygon, but coordinates to the Zn ions in a monodentate fashion. Whereas the sulfur atoms of the thiophene moieties are facing in a head-to-head fashion in **2** (Fig. 3c), those in **1** are flipped over to face in a head-to-tail fashion (Fig. 3a). Despite the similarity of the coordination environments of the Zn atoms in both **1** and **2**, the conformational difference of the thdc is the key in differentiating the dimensionality of the resulting framework structures, and leads to the framework polymorphism.

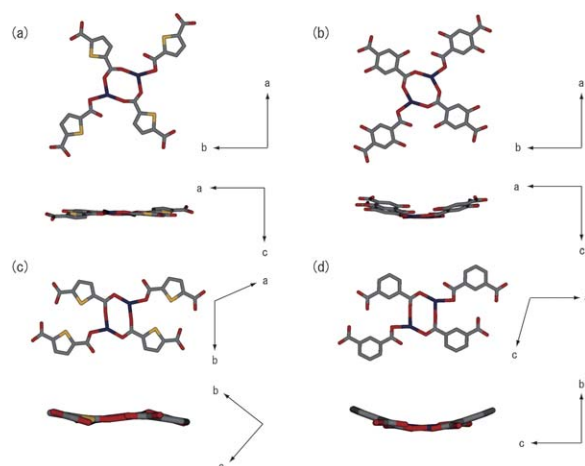


**Fig. 3** Coordination environment of Zn(II) ion for (a) **1**·DMF, (b) reported PCP;  $\{[\text{Zn}(\text{dhytpa})(\text{bpy})]\cdot 4\text{DMF}\}_n$ , (c) **2**·DMF·MeOH and (d) reported PCP;  $\{[\text{Zn}_2(\text{isa})_2(\text{bpy})_2]\text{DMF}\}_n$ .

Unfortunately, the framework structure of **1** was not stable enough to preserve its crystallinity after the removal of the guest molecules, which made it difficult to elucidate its gas adsorption properties. However, we obtained guest-free crystalline samples of **2**. Adsorption measurements of **2** were carried out for  $\text{CO}_2$ ,  $\text{N}_2$ , and  $\text{O}_2$ , as shown in Fig. 4. A series of CID compounds has been reported to show selective guest adsorption properties, thanks to their structural flexibility and the hydrophobicity of the pore surface.<sup>9</sup> Moreover, a highly selective adsorption of  $\text{CO}_2$  from a ternary mixture of  $\text{O}_2$ ,  $\text{N}_2$ , and  $\text{CO}_2$  has been demonstrated.<sup>10</sup> As shown in Fig. 4, the adsorption isotherms show a steep uptake for  $\text{CO}_2$  and  $\text{O}_2$  at low relative pressures, but a gradual uptake for  $\text{N}_2$ . This gradual adsorption for  $\text{N}_2$  suggests a slower diffusion of  $\text{N}_2$  molecules in the pores. In general, CID frameworks either do not adsorb  $\text{N}_2$  or show a gate-opening phenomenon at 77 K because of their intrinsically small pores. In this study, for the first time, we have elongated the diamine linker from bpy to dpNDI, giving rise to a larger channel structure. Even though a slower diffusion rate was observed, the framework of **2** accommodated a significant amount of  $\text{N}_2$  molecules. Note that compared with the saturated adsorption amount for  $\text{CO}_2$  and  $\text{N}_2$  ( $112 \text{ cm}^3 \text{ g}^{-1}$  (STP)), a significant increase in  $\text{O}_2$  uptake ( $174 \text{ cm}^3 \text{ g}^{-1}$  (STP)) was observed with a step at  $P/P_0 = 0.01$ . The adsorption amount of  $\text{O}_2$  at this pressure is comparable to the saturated adsorption amounts of  $\text{CO}_2$  and  $\text{N}_2$  (Fig. 4b). Further  $\text{O}_2$  uptake over  $P/P_0 = 0.01$  suggests that the structural transformation of **2** induces further pore opening, resulting in an increase in  $\text{O}_2$  adsorption. The specific interactions between the framework and the  $\text{O}_2$  molecules may be important for the guest-selective structural change,<sup>13</sup> although the reason remains unclear.

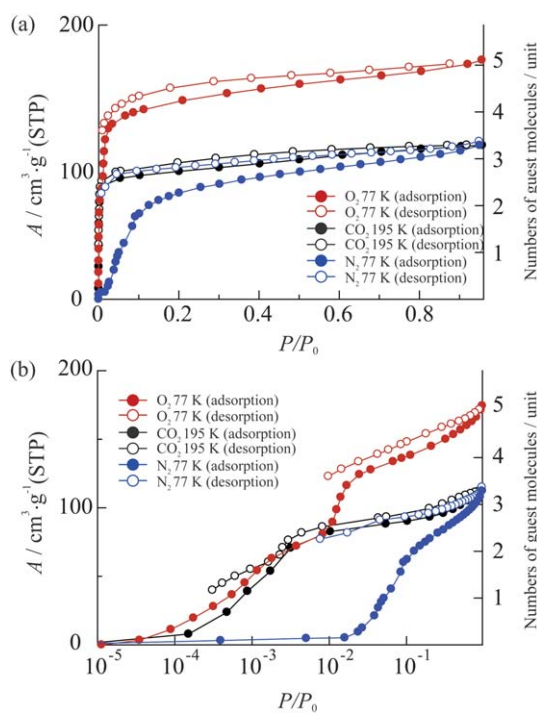


**Fig. 4** (a) Adsorption (filled circles) and desorption (open circles) isotherms of **2** for  $\text{O}_2$  (red) at 77 K,  $\text{CO}_2$  (black) at 195 K and  $\text{N}_2$  (blue) at 77 K. (b) Adsorption and desorption isotherms plotted against the logarithmic relative pressure.

Finally, we elucidated the CT character between the NDI moiety of the framework and aromatic guest molecules with an electron-donating ability. Three different donating guest molecules, anisole, 1,2-dimethoxybenzene (DMB), and *N,N*-dimethylaniline (NDMA), were successfully incorporated into the pores of both **1** and **2** using a guest-exchange protocol, where the as-synthesized samples were soaked in a liquid of each of the guest molecules. As shown in Fig. 5, the electronic absorption spectrum of each sample was measured. In all cases, the characteristic CT transition band was observed in the visible light region, resulting in a color change of the crystalline sample. A red shift in the CT transition band was observed in both **1** and **2** on increasing the donating ability of the guest molecules from anisole to NDMA. For anisole and NDMA, both frameworks exhibited similar spectra as well as resulting colors: yellow for anisole and violet for NDMA. By contrast, the interaction of NDI with DMB gives different colors: red for **1**–DMB and orange for **2**–DMB, which indicate that the CT interaction of NDI with DMB in **1** was stronger than that in **2**.

Powder X-ray diffraction (PXRD) measurements were carried out on all the samples to determine the structural transformations in response to the guest molecule exchange. The PXRD patterns of **1**–guest showed significant shifts of the 110 and 200 diffractions peaks on accommodating the aromatic guest molecules, compared to the as-synthesized framework of **1**–DMF (see ESI†, Fig. S4). Because no shift in the 002 diffraction peaks was observed, the 2D layer structure exhibited a shearing transformation in the *ab* plane to efficiently trap and interact with the aromatic donor molecules and to enhance the CT interaction. On the other hand, all the XRD patterns of **2**–guest look similar, showing the very small structural change in response to the guest molecule exchange. The less framework

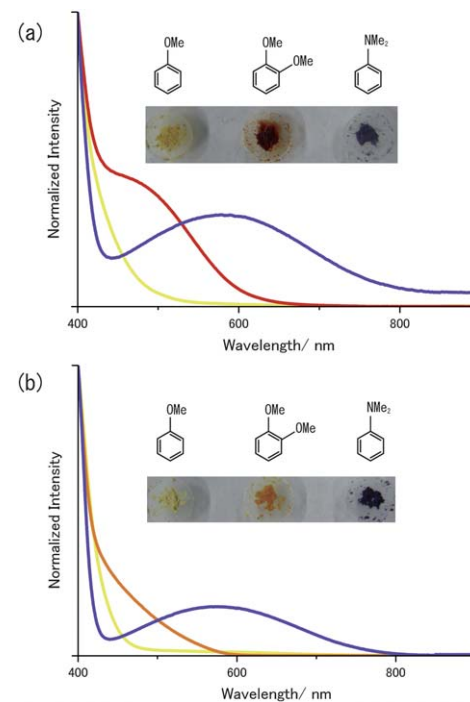


**Fig. 5** Diffuse reflectance UV-Vis spectra of (a) **1**–anisole (yellow), **1**–DMB (red line) and **1**–NDMA (purple line), and (b) **2**–anisole (yellow line), **2**–DMB (orange line) and **2**–NDMA (purple line). Photographs of their samples are shown in the graph.

flexibility of **2** most likely makes it difficult to especially interact with sterically bulky DMB, resulting in a less enhanced charge-transfer transition band in the electronic absorption spectrum.

In conclusion, we have synthesized the framework isomers of redox-active and flexible PCPs,  $[Zn(thdc)(dpNDI)]_n$ , using dpNDI as the electron-accepting ligand and thdc as the topology-directing ligand. The unique connecting angle of thdc promotes the formation of either a 3D pillared-layer framework or an interdigitated 2D layer framework, which are originally synthesized with terephthalic acid or isophthalic acid, respectively. Furthermore, these isomers show different CT interactions with electron-donating aromatic molecules because of their intrinsic porous structure determined by their topology. Such topological design of PCPs can be used in guest-selective sensor materials.

## Acknowledgements

We acknowledge Dr Satoshi Horike and Mr Tomohiro Fukushima for fruitful discussion.

## Notes and references

‡ Crystal data for **1**  $\supset$  DMF:  $C_{30}H_{14}N_4O_8S Zn$   $M_r = 655.91$ , monoclinic, space group  $P2_1/a$ , (#14),  $a = 17.615(5)$  Å,  $b = 16.644(5)$  Å,  $c = 19.660(5)$  Å,  $\beta = 91.890(5)$ ,  $V = 5761(3)$  Å $^3$ ,  $Z = 4$ ,  $T = 223(2)$  K,  $\rho_{\text{calcd}} = 0.756$  Mg m $^{-3}$ ,  $\mu(\text{MoK}\alpha) = 2.994$  cm $^{-1}$ ,  $2\theta_{\text{max}} = 55.0^\circ$ ,  $\lambda(\text{MoK}\alpha) = 0.71069$  Å, 60 561 reflections measured, 13 398 unique ( $R_{\text{int}} = 0.1213$ ), 7775 ( $I > 2\sigma(I)$ ) were used to refine 397 parameters,  $wR_2 = 0.1911$  ( $I > 2\sigma(I)$ ),  $R_1 = 0.0643$  ( $I > 2\sigma(I)$ ), GOF = 0.880. CCDC 782568.

Crystal data for **2**  $\supset$  DMF·MeOH:  $C_{30}H_{14}N_4O_8S Zn$   $M_r = 655.91$ , triclinic, space group  $P\bar{1}$ , (#2),  $a = 10.373(6)$  Å,  $b = 11.875(7)$  Å,  $c = 15.088(9)$  Å,  $\alpha = 93.108(7)$ ,  $\beta = 104.184(5)$ ,  $\gamma = 105.905(6)$ ,  $V = 1718.2$  (17) Å $^3$ ,  $Z = 2$ ,  $T = 93(2)$  K,  $\rho_{\text{calcd}} = 1.214$  Mg m $^{-3}$ ,  $\mu(\text{MoK}\alpha) = 2.994$  cm $^{-1}$ ,  $2\theta_{\text{max}} = 55.0^\circ$ ,  $\lambda(\text{MoK}\alpha) = 0.71069$  Å, 19 158 reflections measured, 7742 unique ( $R_{\text{int}} = 0.0818$ ), 5156 ( $I > 2\sigma(I)$ ) were used to refine 397 parameters,  $wR_2 = 0.2183$  ( $I > 2\sigma(I)$ ),  $R_1 = 0.0757$  ( $I > 2\sigma(I)$ ), GOF = 1.020. CCDC 782567.

1 (a) O. M. Yaghi, M. O'Keeffe, N. W. Ockwig, H. K. Chae, M. Eddaoudi and J. Kim, *Nature*, 2003, **423**, 705; (b) S. Kitagawa, R. Kitaura and S. Noro, *Angew. Chem., Int. Ed.*, 2004, **43**, 2334; (c) G. Férey, C. Mellot-Draznieks, C. Serre and F. Millange, *Acc. Chem. Res.*, 2005, **38**, 217; (d) D. Bradshaw, J. B. Claridge, E. J. Cussen, T. J. Prior and M. J. Rosseinsky, *Acc. Chem. Res.*, 2005, **38**, 273; (e) R. E. Morris and P. S. Wheatley, *Angew. Chem., Int. Ed.*, 2008, **47**, 4966; (f) Z. Wang and S. M. Cohen, *Chem. Soc. Rev.*, 2009, **38**, 1315–1329; (g) D. Zacher, O. Shekhah, C. Wöll and R. A. Fischer, *Chem. Soc. Rev.*, 2009, **38**, 1418–1429.

2 (a) M. Kondo, T. Yoshitomi, K. Seki, H. Matsuzaka and S. Kitagawa, *Angew. Chem., Int. Ed. Engl.*, 1997, **36**, 1725; (b) J. L. C. Rowsell, A. R. Millward and O. M. Yaghi, *J. Am. Chem. Soc.*, 2004, **126**, 5666; (c) A. R. Millward and O. M. Yaghi, *J. Am. Chem. Soc.*, 2005, **127**, 17998.

3 (a) J. Li, R. J. Kuppler and H. Zhou, *Chem. Soc. Rev.*, 2009, **38**, 1477; (b) S. Couck, J. F. M. Denayer, G. V. Baron, T. Remy, J. Gascon and F. Kapteijin, *J. Am. Chem. Soc.*, 2009, **131**, 6326.

4 M. Dincă and J. R. Long, *Angew. Chem., Int. Ed.*, 2008, **47**, 6766.

5 R. Matsuda, R. Kitaura, S. Kitagawa, Y. Kubota, R. V. Belosludov, T. C. Kobayashi, H. Sakamoto, T. Chiba, M. Takata, Y. Kawazoe and Y. Mita, *Nature*, 2005, **436**, 238.

6 (a) H. Li, M. Eddaoudi, T. L. Groy and O. M. Yaghi, *J. Am. Chem. Soc.*, 1998, **120**, 8571; (b) A. R. Millward and O. M. Yaghi, *J. Am. Chem. Soc.*, 2005, **127**, 17998.

7 (a) O. Ohmori, M. Kawano and M. Fujita, *J. Am. Chem. Soc.*, 2004, **126**, 16292; (b) S. Shimomura, R. Matsuda, T. Tsujino, T. Kawamura and S. Kitagawa, *J. Am. Chem. Soc.*, 2006, **128**, 16416.

8 (a) B. Moulton and M. J. Zaworotko, *Chem. Rev.*, 2001, **101**, 1629; (b) B. Moulton, J. Lu, R. Hajndl, S. Hariharan and M. J. Zaworotko, *Angew. Chem., Int. Ed.*, 2002, **41**, 2821; (c) S. Ma, D. Sun, M. Ambrogio, J. A. Fillinger, S. Parkin and H. Zhou, *J. Am. Chem. Soc.*, 2007, **129**, 1858; (d) S. R. Caskey, A. G. Wong-Foy and A. J. Matzger, *Inorg. Chem.*, 2008, **47**, 7751; (e) S. Bauer, C. Serre, T. Devic, P. Horcajada, J. Marrot, G. Férey and N. Stock, *Inorg. Chem.*, 2008, **47**, 7568; (f) X. Wang, S. Ma, P. M. Forster, D. Yuan, J. Eckert, J. J. López, B. J. Murphy, J. B. Parise and H. Zhou, *Angew. Chem., Int. Ed.*, 2008, **47**, 7263; (g) L. Ma and W. Lin, *J. Am. Chem. Soc.*, 2008, **130**, 13834; (h) D. Sun, S. Ma, J. M. Simmons, J. Li, D. Yuan and H. Zhou, *Chem. Commun.*, 2010, **46**, 1329; (i) D. Sun, Y. Ke, T. M. Mattox, B. A. Ooro and H. Zhou, *Chem. Commun.*, 2005, 5447; (j) J. Zhang, L. Wojtas, R. W. Larsen, M. Eddaoudi and M. J. Zaworotko, *J. Am. Chem. Soc.*, 2009, **131**, 17040.

9 (a) S. Horike, D. Tanaka, K. Nakagawa and S. Kitagawa, *Chem. Commun.*, 2007, 3395; (b) D. Tanaka, K. Nakagawa, M. Higuchi, S. Horike, Y. Kubota, T. C. Kobayashi, M. Takata and S. Kitagawa, *Angew. Chem., Int. Ed.*, 2008, **47**, 3914; (c) T. Fukushima, S. Horike, Y. Inubushi, K. Nakagawa, Y. Kubota, M. Takata and S. Kitagawa, *Angew. Chem., Int. Ed.*, 2010, **49**, 4820.

10 K. Nakagawa, D. Tanaka, S. Horike, S. Shimomura, M. Higuchi and S. Kitagawa, *Chem. Commun.*, 2010, **46**, 4258.

11 (a) G. Andric, J. F. Boas, A. M. Bond, G. D. Fallon, K. P. Ghiggino, C. F. Hogan, J. A. Hutchison, M. A. Lee, S. J. Langford, J. R. Pilbrow, G. J. Troup and C. P. Woodward, *Aust. J. Chem.*, 2004, **57**, 1011; (b) J. J. Reczek, K. R. Villazor, V. Lynch, T. M. Swager and B. L. Iverson, *J. Am. Chem. Soc.*, 2006, **128**, 7995; (c) E. Takahashi, H. Takaya and T. Naota, *Chem.-Eur. J.*, 2010, **16**, 4793; (d) Y. Takashima, V. M. Martinez, S. Furukawa, M. Kondo, S. Shimomura, H. Uehara, M. Nakahama, K. Sugimoto and S. Kitagawa, *Nat. Commun.*, 2011, **2**, 168, DOI: 10.1038/ncomms1170.

12 T. Yamada and H. Kitagawa, *J. Am. Chem. Soc.*, 2009, **131**, 6312.

13 M. S. A. Abdou, F. P. Orfino, Y. Son and S. Holdcroft, *J. Am. Chem. Soc.*, 1997, **119**, 4518.